CHEMISTRY
A European Journal

A Journal of
ChemPubSoc Europe

Accepted Article

Title: The structure of linkers affects the DNA binding properties of tethered dinuclear ruthenium (II) metallo-intercalators

Authors: Hiwa Saeed, Ibrahim Saeed, Niklaas Buurma, and Jim Antony Thomas

To be cited as: *Chem. Eur. J.* 10.1002/chem.201605750

Link to VoR: http://dx.doi.org/10.1002/chem.201605750

Supported by
ACES

WILEY-VCH

CHEMISTRY
A EUROPEAN JOURNAL

FULL PAPER

DOI: 10.1002/chem.200((will be filled in by the editorial staff))

The structure of linkers affects the DNA binding properties of tethered dinuclear ruthenium (II) metallo-intercalators

Hiwa K Saeed[a], Ibrahim Q Saeed[b], Niklaas J Buurma[b], and Jim A. Thomas*[a]

Dedication ((optional))

Abstract: With the long-term aim of enhancing the binding properties of dinuclear Ru^{II}-based DNA light-switch complexes, a series of eight structurally related mono- and dinuclear systems are reported in which the linker of the bridging ligand has been modulated. These tethered systems have been designed to explore issues of steric demand at the binding site and the thermodynamic cost of entropy loss upon binding. An analysis of detailed spectroscopic and isothermal titration calorimetry (ITC) studies on the new complexes reveal that one of the linkers produces a dinuclear systems that binds to duplex DNA with an affinity (K_b > 10^7 M^{-1}) that is higher than its corresponding monometallic complex and is the highest affinity for a non-threading bis-intercalating metal complex. These studies confirm that the tether has a major effect on the bindin properties of dinuclear complexe containing nintercalating units an establishes key design rules for th construction of dinuclear complexe with enhanced DNA bindin characteristics.

Keywords: Ruthenium • DNA • luminescence • ITC • intercalation

Introduction

The interactions of metal complexes with biomolecules are attracting increasing attention. [1-10] In this context, the DNA binding properties of $[Ru(phen)_2(dppz)]^{2+}$ (**1**) (phen = 1,10-phenanthroline, dppz = dipyrido[3,2-*a*:2′,3′-*c*]phenazine) – Fig 1 - are of particular interest. [11-13] Although it was long accepted that intercalation of the dppz ligand between base pairs forms the basis of interaction between the complex and duplex DNA, the exact orientation of the DNA bound complex has been much discussed. [14-20] Recently, a series of X-ray crystallography studies on **1** and analogues have confirmed that intercalation of the dppz moiety occurs with the complex in the minor groove, but also revealed that binding is modulated by ancillary ligands as they can bind by "semi-intercalation" in which partial insertion between base pair steps results in considerable bending of the duplex. [21-24] Furthermore, structure obtained from a racemic mixture of **1** reveals that it enantiomers possess subtle differences in their intercalatio geometries. [25]

The optical properties of these systems are particularly attractiv as, since intercalation results in large hypochromicity in th absorption bands of the complex, DNA binding can be monitore using UV-Visible spectroscopy. The luminescent properties of mos Ru(dppz) complexes offer an even more facile means of monitorin binding: although their Ru→dppz ^{3}MLCT-based emission i quenched in water, binding to DNA enhances luminescence b several orders of magnitude – a phenomenon that has becom known as the DNA "light switch" effect.

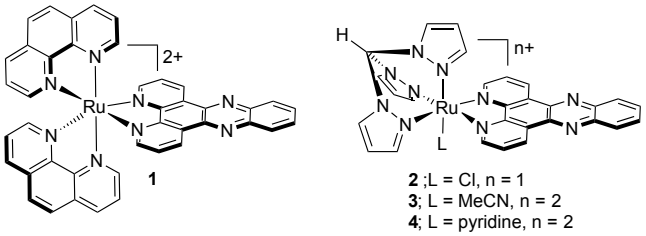

Figure 1. Mononuclear Ru^{II}(dppz) complexes relevant to this report.

Complex **1** and its derivatives are synthesized as racemic mixtures. Although the Λ and Δ enantiomers can be resolved *via* classical or chromatographic procedures, and they do show

[a] Dr H.K. Saeed, Prof J. A. Thomas
Department of Chemistry
University of Sheffield
Sheffield S3 7HF, UK
Fax: (+) 44 114 222 9346
E-mail: james.thomas@sheffield.ac.uk

[b] Mr I. Q. Saeed, Dr N J Buurma
Physical Organic Chemistry Centre, School of Chemistry
Cardiff University
Main Building Park Place, Cardiff CF10 3AT, UK

Supporting information for this article is available on the WWW under http://www.chemeurj.org/ or from the author.

10.1002/chem.201605750

differences in their binding properties and emission lifetimes, the Δ-form shows only modest overall enantioselective DNA binding over its Λ-analogue.[15] Furthermore, the resolved Ru^{II} center in such complexes is coordinately saturated and attempts to modulate their binding properties using ancillary ligands often involves challenging chromatographic separation procedures, or non-trivial modification of already coordinated ligands. [12]

To address both these issues, we have been investigating the properties of achiral $[Ru(tpm)(L)(dppz)]^{n+}$ complexes (tpm = tris(1-pyrazolyl)methane, L = chloride, *N*-donor ligand, *n* =1, 2), which contain an easily modulated coordination site. Using **2** as a precursor, complexes **3** and **4** – Fig 1 - were initially synthesized. The DNA binding parameters of these latter two complexes compare favourably with those of **1** and it was also found that complex **4** has a binding preference for GC sequences of DNA. [26] Using the same building block, bimetallic systems have been investigated.

From first principles, ditopic substrates should bind more extended DNA sequences compared to similar mononuclear systems[27,28] and indeed the number of studies investigating the DNA binding and biological properties of oligonuclear metal complexes is rapidly growing.[29-37] Of particular relevance to this report, Keene and Collins have shown that dinuclear Ru^{II} complexes that bind nucleic acids through groove binding offer considerable potential as therapeutic leads. [38-42]

Nevertheless, due to the synthetic difficulties discussed above, bisintercalating systems incorporating Ru units are still relatively rare. [43-45] The best-characterized systems are those reported by Lincoln, *at al*., in which bridging ligands containing linked dppz units have been used to create threading intercalators. [46-50] Due to the threading mechanism, [51] the resulting dinuclear complexes show extremely high binding affinities (in the nanomolar range) [52] and a binding preference for AT rich sequences. [50,53] On the other hand, the multi-step syntheses of these complexes starting from classically resolved chiral metal complex starting materials are not trivial.

In contrast, using complex **2** as a starting point, we have shown that dinuclear systems incorporating $[Ru(tpm)(dppz)]^{2+}$ moieties linked by a ditopic dipyridyl ligands can be readily prepared in two steps using the intermediate complex **5**. This approach provided a simple route to homo and – for the first time - heterometallic M(dppz) systems such as **6** and **7** – Scheme 1. [54-56] Disappointingly, although these systems bind to extended sequences and display unique photophysical properties, they do not show enhanced DNA-binding compared to their analogous monometallic analogues. A possible reason for this observation involves the nature of the tether employed: isothermal calorimetric studies on **6** indicated that the favourable binding entropy for the tethered dinuclear system is lower than expected which was attributed to loss in the degrees of freedom available to the bound linker.

In related studies, we found that the DNA binding affinities of mononuclear $Ru(tpm)(pyNH_2)(dppz)]^{n+}$ complexes (where $pyNH_2$ = 3- or 4-amino pyridine) are greatly affected by the positioning of substituents on the pyridine ligand. Although the 3-$pyNH_2$-based complex binds by intercalation with affinities that are comparable to the parent compound, the coordinated 4-$pyNH_2$ complex is a low affinity, non-intercalating, groove binder. NMR studies revealed that this is due to unfavourable interactions made by the 4-NH_2 of the coordinated pyridine projecting into the minor groove of the duplex.[57,58] This suggests that 4-py-based connectivity within the tether of **6** may have an unfavourable effect on its binding characteristics.

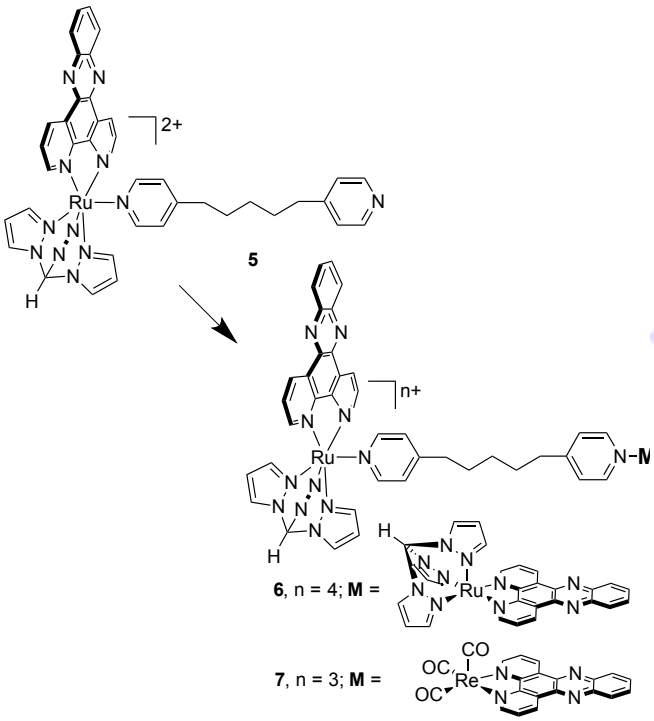

Scheme 1. Previously studied dinuclear complexes incorporating the Ru^{II}(tpm)(dppz moiety synthesized from mononuclear complex **5**.

Therefore, with the long term aim of optimizing the DNA binding properties of oligonuclear $[Ru(tpm)(dppz)]^{2+}$ complexes an ascertaining how the nature of the tether affects binding properties we have prepared four connecting ligands that possess potentia DNA recognition sites in themselves. The ligands, which have als been chosen to investigate the effects of changes in connectivity an linker rigidity on the binding properties of metallo-intercalators have then been used to synthesize four new mononuclear and fou new dinuclear complexes. The duplex DNA binding properties c these new complexes were then parameterised and compared to eac other and their mononuclear analogues using a variety c biophysical techniques.

Results and Discussion

Synthetic studies. The four new pyridine-based bridging ligand were prepared in high yield by reduction of the corresponding Schiff base ligands with $NaBH_4$. The py-X-py linkers were prepared in a one-pot reaction in ethanol, whilst linkers py-Y-py were prepared in two steps through the condensation of benzene-1,4-dicarboxaldehyde and the appropriate (aminomethyl)pyridine yielding a Schiff base which was reduced with $NaBH_4$ in ethanol to afford the desired linker.

Monomer Ru^{II} complexes were then obtained by first removing the chlorido ligand of $[(tpm)Ru(dppz)(Cl)]PF_6$ using Ag^+ and then adding an excess of the required dipyridyl linker ligand. Using this

10.1002/chem.201605750

method, complexes **8**, and **10** incorporating the tether ligands *N,N*'-bis(4-pyridylmethyl)-1,6-hexanediamine (4py-X-4py) and *N,N*'-bis(4-pyridylmethyl)-1,4-benzenedimethyleneamine (4py-Y-4py), were obtained. Using isomeric tethers *N,N*'-bis(3-pyridylmethyl)-1,6-hexanediamine (3py-X-3py) and *N,N*'-bis(3-pyridylmethyl)-1,4-benzenedimethyleneamine (3py-Y-3py) complexes **12**, and **14** were isolated through similar methods – Figure 2. All four tethers possess amino groups within their linker unit as this mimics the recognition motif of polyamines such as spermine and spermidine that bind non-specifically - but with high affinity - to nucleic acids through electrostatic interactions.[59]

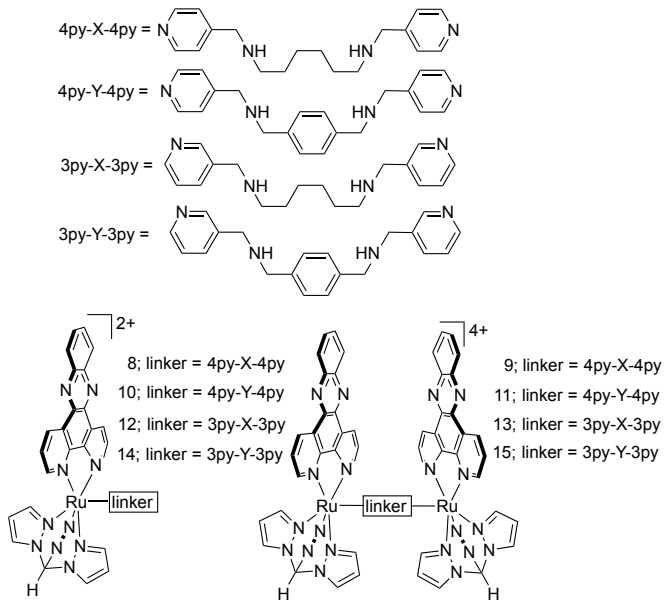

Figure 2. New ditopic ligands, mono-, and dinuclear Ru(dppz) complexes reported in this study.

Using the same methods outlined in Scheme 1, the mononuclear complexes were then used to synthesize analogous dinuclear systems $[\{Ru(tpm)(dppz)\}_2(4py\text{-}X\text{-}4py)]^{4+}$ (**9**), $[\{Ru(tpm)(dppz)\}_2(\mu\text{-}4py\text{-}Y\text{-}4py)]^{4+}$ (**11**), $[\{Ru(tpm)(dppz)\}_2(3py\text{-}X\text{-}3py)]^{4+}$ (**13**), and $[\{Ru(tpm)(dppz)\}_2(3py\text{-}Y\text{-}3py)]^{4+}$ (**15**) - Fig 2. Analytically pure dinuclear complexes could then be obtained through ion-exchange chromatography.

Photophysical studies. The photophysical properties of **8 - 15** as hexafluorophosphate salts in acetonitrile are summarized in Table 1. The UV−Visible spectra of the complexes are dominated by high-energy bands between 270−300 nm which correspond to π→π* transitions of the aromatic nitrogen donor ligands. The UV−Visible spectrum of the dppz ligand in acetonitrile exhibits a moderately intense band in the near-UV with two principal maxima at λ = 358 and 376 nm, which are characteristic of π→π*(dppz) transitions. [60] Consequently, the moderately intense bands in the near-UV regions for complexes **8** (351 nm), **9** (353 and 401 nm), **10** (352 nm) and **11** (355 and 407 nm) are assigned to analogous transitions.

The MLCT Ru(dπ)→dppz(π*) ^{1}MLCT bands for **8**−**15** all appear in the region of the spectrum typical for ruthenium(II) complexes with coordinated polyimine ligands, although the dinuclear complexes are slightly red shifted by 20 - 30 nm compared to their corresponding mononuclear systems. Excitation into the MLCT band of the complexes results in the characteristic broad and unstructured emission originating from the Ru(dπ)→dppz(π*) ^{3}MLCT manifold, see Table 1. Depending on the complex, the energy of this emission ranged from around λ_{em} = 635 - 661 nm.

DNA Binding Studies.

Water-soluble chloride salts of all eight complexes were obtained *via* anion metathesis of their respective PF_6^- salts using $[n\text{Bu}_4\text{N}]\text{Cl}$ in acetone. Their interaction with CT-DNA in aqueous buffer (25 mM NaCl, 5 mmol tris, pH 7.4) was then investigated using UV–visible and emission spectroscopic titrations.

Table 1. Room temperature photophysical properties of **8** − **15** as hexafluorophosphate salts in acetonitrile.

	Absorption	Emission	
Complex	Λ / nm (10^{-3}ε / M^{-1} cm^{-1})	λ_{ex} / nm	λ_{em} / nm
	Mononuclear complexes		
8	278 (55.4), 317 (19.5), 351 (20.3), 401 (8.3), 431 (6.5), 494 (2.8)	420	661
10	278 (55.4), 317 (20.0), 350 (21.1), 401 (8.9), 431 (6.9), 491 (3.1)	430	659
12	232 (22.0), 278 (38.5), 319 (10.7), 357 (13.1), 401 (5.9), 441 (3.6), 501 (1.6)	440	644
14	226 (24.7), 278 (30.9), 319 (14.4), 355 (12.7), 401 (6.8), 435 (3.8), 496 (1.5)	430	639
	Dinuclear Complexes		
9	276 (100.3), 318 (29.6), 355 (25.9), 368 (23.0), 468 (7.7)	440	630
11	278 (59.4), 317 (20.5), 351 (21.2), 401(8.9), 431(6.0), 494(3.3)	460	661
13	227 (20.6), 279 (47.3), 319 (13.2), 359 (18.2), 403 (8.1), 433 (5.6), 498 (2.2)	433	642
15	229 (31.2), 278 (67.5), 317 (19.4), 357 (19.8), 411 (9.5), 501 (3.7)	417	635

Optically based titrations. On addition of CT-DNA both the absorption and emission spectra of the complexes produced changes that are characteristic of DNA binding. Large hypochromicity in both π→π* and MLCT absorption bands are observed, Fig 3a, such shifts are often ascribed to an intercalative binding mode. As expected, although all the complexes are essentially non-luminescent in aqueous solutions, on addition of DNA, their Ru^{II}→dppz based ^{3}MLCT emission is greatly enhanced – Fig 3b. This change is similar in magnitude for all the complexes, with

10.1002/chem.201605750

emission enhancements of x90 – 100 being observed. Since the mono- and dinuclear complexes display almost identical light switch effects on binding to DNA, it seems *each* Ru(dppz) unit of the dinuclear complexes is isolated from bulk solvent to the same extent as their corresponding mononuclear complex. Thus, it is tempting to conclude that the dinuclear complexes bis-intercalate into DNA, however a number of previous studies have shown that full intercalation is not always required for a light-switch effect to operate. [61-64]

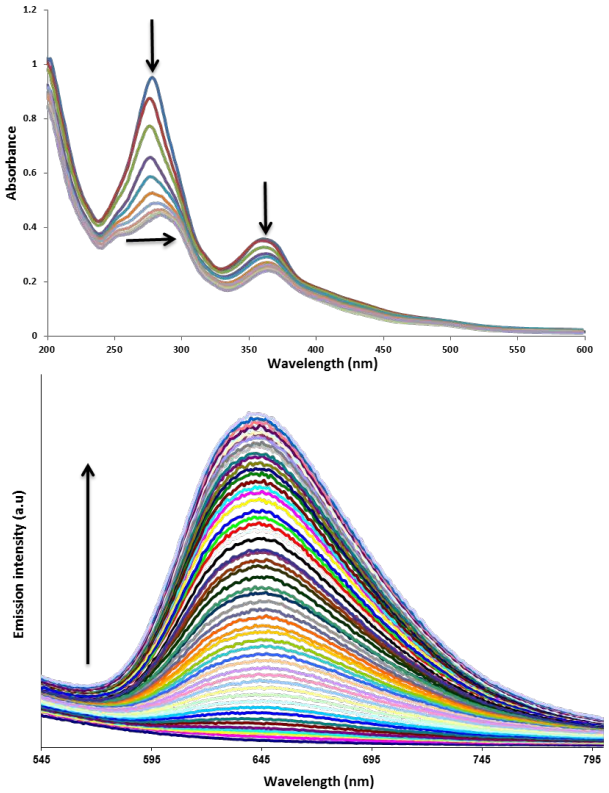

Figure 3. Details in changes in the UV-visible (A) and luminescence (B) spectra of 15 μM complex **9** on progressive addition of CT-DNA in 5 mM tris buffer, 25 mM NaCl, pH 7.4 at 25 °C.

Unfortunately, whilst both the absorption and emission data produce what appear to be typical binding curves, fits of either sets of titrations to the much-used McGhee-von Hippel model[65] for a single non-cooperative binding mode to the data were poorly correlated, suggesting more complex binding behaviour, possibly as a result of the heterogeneity of the binding sites on CT-DNA. Nevertheless, the UV-visible spectroscopic titrations could be analysed in terms of the multiple independent binding sites, MIS, model. Our version of the MIS model [66] explicitly takes the ligand concentration into account – see SI for details - and thus avoids the need to keep the ligand concentration constant upon addition of DNA. As Figure 4 shows, the MIS model reproduces the data very well, despite the sequence heterogeneity of the CT-DNA used. Again, it should be noted that this does not necessarily indicate a single class of binding sites, as we have observed similarly good fits of the MIS model to nucleic acid binders, which actually display multiple binding modes when studied by ITC. [66] Therefore the quality of the observed fit cannot be used to conclude that binding is to a single class of sites. Taking this caveat in mind, we report apparent binding parameters in Table 2. This analysis also results in apparent binding sites with an average size of 2.2±1.0 base pairs.

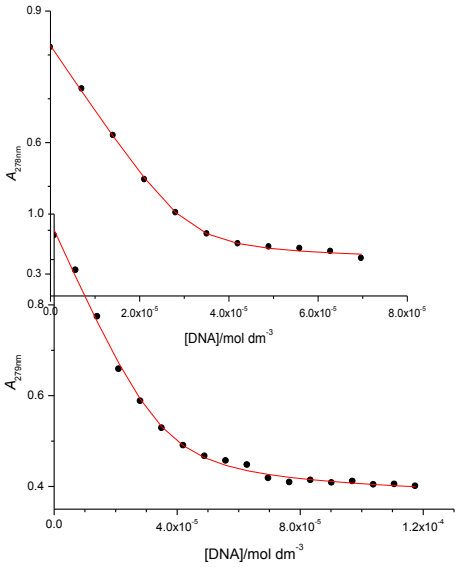

Figure 4. Examples of fits of the MIS model to the UV-Visible spectroscopic titratic data. Top: complex **8**, bottom: complex **9**. In both cases: • = data, — = fit

Table 2. Apparent binding parameters from fitting the MIS model to UV-visible data fo **8-15** interacting with CT-DNA at 25 °C in 5 mM Tris, 25 mM NaCl, pH 7.4

complex	K / 10^6 M^{-1}	binding site / b.p.	ε / 10^3 M^{-1}cm^{-1}	$\Delta\varepsilon$ / 10^4 M^{-1}cm^{-1}	λ / nm
		Mononuclear complexes			
8	2.2±0.7	2.1±0.1	54.8	-3.19	278
10	0.7±0.3	1.9±0.2	51.8	-3.05	276
12	0.12±0.05	1.1±0.3	38.2	-2.58	280
14	6.9±3.4	1.9±0.1	52.2	-2.65	280
		Dinuclear complexes			
9	0.9±0.3	2.4±0.2	64.3	-3.77	279
11	0.2±0.1	1.1±0.3	45.1	-2.71	279
13	1.7±0.6	4.6±0.3	75.1	-7.1[a]	268
15	2.5±0.8	2.1±0.1	66.9	-3.59	278

a) $\Delta\varepsilon$ restricted to values lower than ε.

Despite the good fits and the typically reasonable binding site sizes, the MIS model may not be a complete model for the interactions between **8-15** and CT-DNA. For example, its sequence heterogeneity means that CT-DNA may contain a number of binding sites for which the studied complexes display a range of affinities. In addition, non-specific electrostatic interactions may further affect the spectroscopic data.[68] Therefore estimates from fits to this model probably define the lower limit of DNA binding affinities. Despite this limitation, these estimates reveal some striking trends. Although the apparent K_b values for the dinuclear

10.1002/chem.201605750

complexes still appear to be comparable or slightly lower to their corresponding mononuclear complexes, it is clear that the nature of the tether *does* affect the binding properties of the complexes, with complexes **14** and **15** - which both contain the py-Y-py linker - displaying affinities that are up to an order of magnitude larger than complexes **5** – **13**. Viscosity studies were used to explore this issue in more detail.

Viscosity Studies. Viscosity measurements provide a convenient method to confirm DNA binding modes. In particular, intercalation leads to a lengthening of DNA, thus producing an easily detected concomitant increase in the relative viscosity of DNA solutions, while groove binding does not cause such effects.[67-69] Viscosity experiments on **8** – **15** (Figure 5) revealed distinctive variance between complexes with different ligand connectivity.

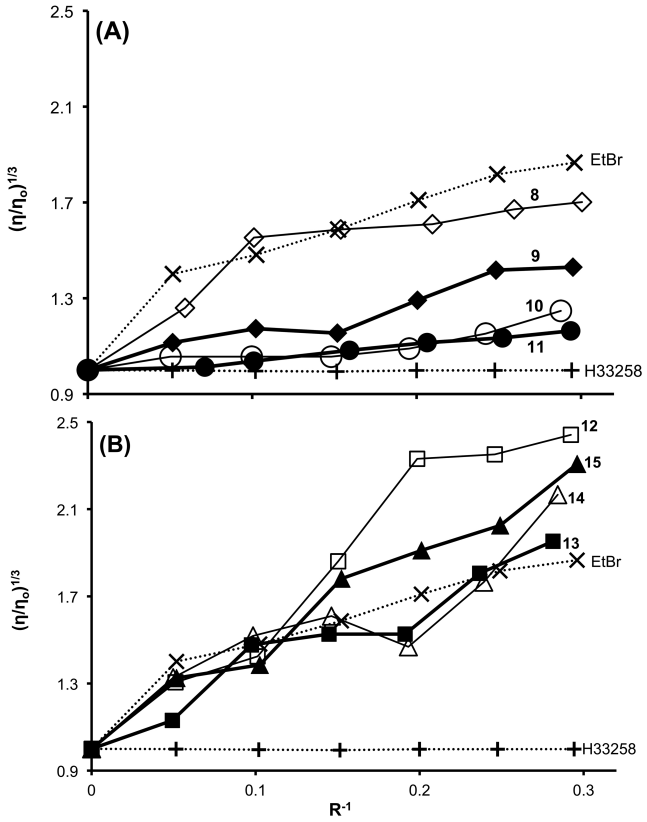

Figure 5. Relative viscosity changes in CT-DNA solutions on addition of (A) complexes **8** – **11** and (B) complexes **9** – **15**. For ease of comparison changes induced by the groove binder H33258 and intercalator EtBr under the same conditions are also included.

Although additions of 4-py complexes **8** – **11** to CT-DNA solutions produce a positive increase in viscosity, their effect is smaller than that of the confirmed, nonspecific, intercalator ethidium bromide, EtBr. Furthermore, comparisons between the complexes show that the dinuclear complexes produce less change in viscosity than their corresponding mononuclear analogues; it is also apparent that complexes **10** and **11**, which incorporate the less flexible 4py-Y-4py tether, induce less change than the 4py-X-4py-based complexes **8** and **9** - Fig 5a.

In contrast, additions of 3-py complexes **12** – **15** induce viscosity changes that are significantly larger than those induced by EtBr and although mononuclear complex **12** induces a larger increase than its dinuclear analogue **13**, a comparison between the two complexes coordinated to the more rigid 3py-Y-3py tether shows that dinuclear complex **15** now actually induces *larger* changes than mononuclear complex **14** – Fig 5b.

These observations suggest that, due to reduced unfavourable steric interactions of 3-py complexes with the duplex, complexes **12** - **15** are deeper, more effective intercalators than **8** – **11**; however the possibility that the latter systems are more selective and bind at specific sites within a sequence cannot be discounted as this would also produce a lower overall lengthening of the DNA. Nevertheless, again, it is clear that the nature of the linker has a profound effect on the DNA interactions of these new complexes. To parameterize these effects in more detail isothermal calorimetry, ITC experiments were carried out.

Isothermal calorimetry studies. For all the new complexes binding thermodynamics with DNA at 25 °C were determined by ITC. First, the heat effects for dilution were determined (not shown) and these were found to be constant, an observation that indicates that **8**-**15** do not aggregate significantly under the experimental conditions; consequently, titrations with CT- DNA were then carried out.

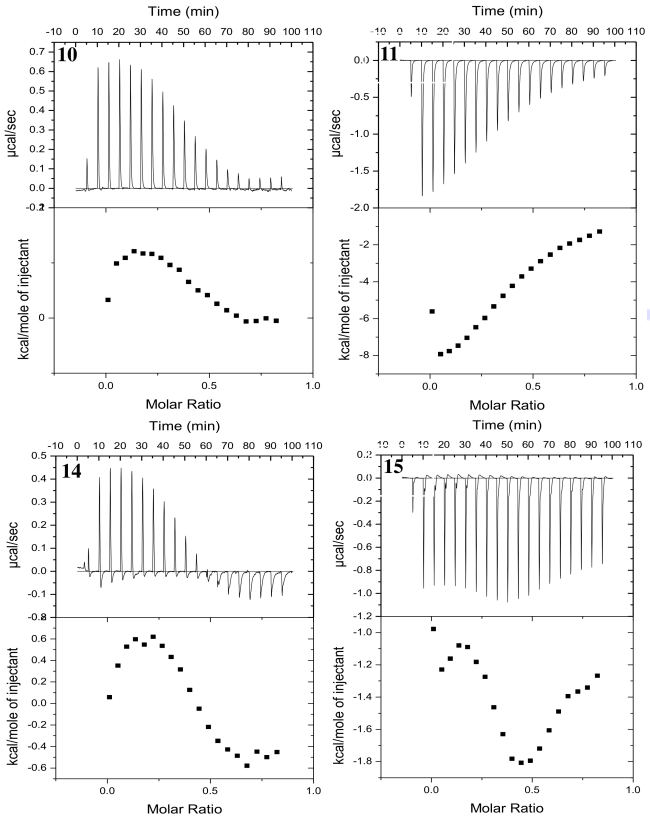

Figure 6. Enthalpograms for the interaction of **10**, **11**, **14** and **15** with CT-DNA at 25 °C in 5 mM Tris, 25 mM NaCl, pH 7.4.

As shown in Figure 6, several of the titrations exhibit non-constant heat effects before a main sigmoidal transition around a molar ratio of 0.3 corresponding to saturation of binding sites. These non-constant heat effects are typical of multiple simultaneous equilibria in which binding affinities are very close in magnitude.[70] Again, the presence of such binding sites is not surprising

considering the heterogeneity of the CT-DNA sequence and is broad agreement with the data derived from UV-visible titrations (*vide supra*). The binding isotherm for **15**, however, shows two clear sigmoidal transitions, one around a molar ratio of 0.3 and one around a molar ratio of 0.6. These transitions are clearly indicative of two binding events with well-defined and significantly different binding affinities.

Figure 6 also shows that the observed heat effects are generally rather small, which is not uncommon for binding events involving a significant contribution from hydrophobic interactions.[71] DNA binding of **8** - **10** and **12** - **14** is slightly endothermic but the interaction of **11** with CT-DNA is strongly exothermic, while the interaction of **15** with CT-DNA displays an exothermic event as well.

To obtain binding parameters, and evaluate the significance of the obtained values, the enthalpograms were analysed using the in-house software packages ICITC and I2CITC.[72,73] Typically, statistically significant values could only be determined for the main transitions, i.e. the binding events with stoichiometries around 0.3, and these are summarized in Tables 3 and 4.

Table 3**.** Summary of binding parameters for the main binding mode of 4-py-based complexes **8** – **11** interacting with CT-DNA at 25 °C in 5 mM Tris, 25 mM NaCl, pH 7.4 from ITC.

Complex	**8**	**9**	**10**	**11**
equilibria in fit	1	2[a]	2[a]	1
K_b / M^{-1}	6.4×10^5	1.6×10^5	1.5×10^5	1.0×10^5
S / bp	3.7	2.8	2.8	2.4
ΔH / kJ mol^{-1}	10.8	8.2	6.4	-39.4
$-T\Delta S$ / kJ mol^{-1}	-43.9	-32.5	-35.8	+11
ΔG / kJ mol^{-1}	-33.1	-29.7	-29.4	-28.4

[a] n for the first equilibrium was restricted to the range [0.0002 – 0.2] ligands per base pair, i.e. S was restricted to the range [5-5000] base pairs.

Table 3 shows the thermodynamic parameters for binding of the first group of complexes, **8** – **11**, involving 4-py linkages. These data do not allow quantification of the binding parameters for the first binding events for **9** and **10** because of extensive parameter correlation. This inability to unambiguously quantify the first binding events is expected, as the enthalpograms do not display a clear sigmoidal transition from one binding event to the next.

The quantified interactions of **8** – **10** display a very similar thermodynamic signature, as they are all slightly endothermic with entropy driven binding. Strikingly, as is already obvious from the form of the enthalpograms, dinuclear complex **11** shows a very different thermodynamic profile, with binding being enthalpy driven and entropy opposed. Within this group, binding constants for the dominant mode for the dinuclear complexes is lower than that for the corresponding monomeric complex, while the binding site size remains more or less constant. The interaction parameters thus indicate that the affinities of the dinuclear complexes are not increased through multivalency. Moreover, it is clear that in both cases the reduced affinity of the bisintercalator is due to a lower favourable entropic contribution to binding. These observations are consistent with our previous ITC studies on complexes **5** and **6**.

Table 4. Summary of binding parameters for 3-py-based complexes **12** – **15** interacting with CT-DNA at 25 °C in 5 mM Tris, 25 mM NaCl, pH 7.4 from ITC.

Complex	**12**	**13**	**14**	**15**
equilibria in fit	2	1	2	2
K_b1 / M^{-1}	-[a]	1.9×10^5	-[a]	2.7×10^7
$S1$ / bp	-[a]	2.1	-[a]	3.3
$\Delta H1$ / kJ mol^{-1}	-[a]	4.0	-[a]	0.6
$-T\Delta S1$ / kJ mol^{-1}	-[a]	-34.1	-[a]	-43.1
$\Delta G1$ / kJ mol^{-1}	-[a]	-30.1	-[a]	-42.5
K_b2 / M^{-1}	1.2×10^5		3.8×10^5	3.5×10^5
$S2$ / bp	2.5		2.7	3.5
$\Delta H2$ / kJ mol^{-1}	7.3		5.1	-2.8
$-T\Delta S2$ / kJ mol^{-1}	-36.3		-37.0	-29.0
$\Delta G2$ / kJ mol^{-1}	-29.0		-31.9	-31.8

[a] not quantifiable based on the available calorimetric data.

The data in Table 4 indicate that - in contrast to their 4-py linke analogues - the 3-py-linked dinuclear complexes display similar c higher affinities for DNA than their corresponding mononuclea complexes, with the estimated K_b for first binding phase for **15** i around two orders of magnitude larger than estimates obtained for and **6** using the same technique.[55] A comparison of the availabl data for **14** and **15** also reveals striking differences: both bindin phases of the dinuclear complex display a more favourable entrop change and a decreased endothermic contribution compared to th data for the mononuclear analogue, indeed the second binding ever between **15** and CT-DNA is actually exothermic. Further analysis c this data is revealing.

Using enthalpy-entropy compensation plots, Chaires has show that groove binders and intercalators DNA have distinctive thermodynamic signatures.[74,75] A similar analysis involving the ITC data shown in Tables 3 and 4 is presented in Figure 7. The data for **8** – **15** are compared to the ITC parameters obtained by Collins and Keene[40] in studies on the minor groove binding complexes shown in the figure.

10.1002/chem.201605750

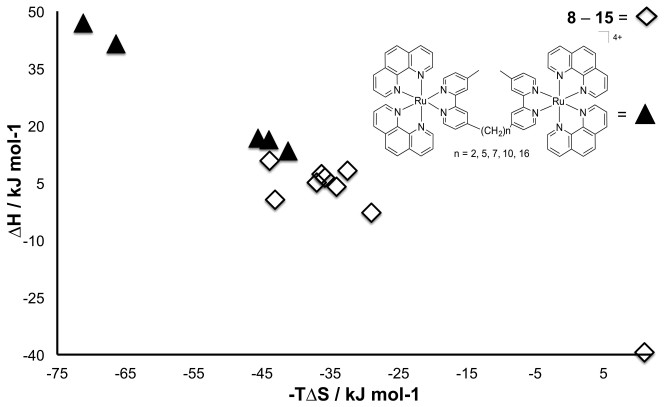

Figure 7. Compensation plot comparing the thermodynamic signatures of complexes **8** – **15** with those of purely minor groove binding complexes reported by Collins and Keene.

In these plots, the two series of complexes can be partitioned into three areas. Unsurprisingly, the purely groove binding complexes reported by Collins and Keene are found in the upper left quadrant, as this interaction is known to be entropically favoured and enthalpically opposed. Sitting in the bottom right quadrant of the plot, the thermodynamic data for **11** is uniquely different as it shows a strongly entropically opposed but enthalpically favoured interaction. This signature is almost identical to a pure intercalator such as ethidium bromide, indicating that there is no binding contribution from the potentially groove binding 4py-Y-4py linker. This is at odds with the observation that **11** produces the smallest increase in the relative viscosity of DNA solutions. As discussed previously these seemingly contradictory observations could be suggestive of a more selective interaction with binding only occurring at specific sites within a sequence. An alternative explanation is that the amino groups of the tether are making specific contacts within a groove, as hydrogen bonding possesses the same observed thermodynamic profile.

Finally, the parameterized binding modes of complexes **8** - **10** and **12** – **15** all display favourable entropies but relatively small enthalpy terms, leading to either slightly endothermic or exothermic interactions; observations that are clearly consistent with mixed, groove binding/intercalative, interactions.

Conclusion

Although the apparent binding parameters derived from the UV-visible titration must be considered with some care, taken together with the viscosity and ITC analysis, it is clear that the nature and the connectivity of the ligand tether has significant effects on the quality and intensity of binding within this series of newly synthesized complexes. In particular, ITC - which makes the availability of multiple different binding sites more obvious and thus allows more direct quantification of the strength of individual interactions - clearly identifies **15** as the most tightly binding system, binding DNA with the highest affinity for a non-threading bis-intercalating metal complex. The ITC data also shows that complex **11** is unique in this series of compounds, as it has an entirely enthalpically driven binding profile, typically seen in "pure" intercalators. Furthermore, all the biophysical studies highlight that the 3py based linkers display enhanced binding compared to their 4py analogues, whilst the ITC data suggests that, in particular, the more rigid and hydrophobic 3py-Y-3py linker contributes favourably to the observed interactions.

These findings show that by optimising linker design for tpm-Ru-based bisintercalators, thermodynamic profiles can be profoundly affected and overall binding affinities significantly enhanced. In particular, the anchor point of pyridine-based tether ligands and the incorporation of recognition sites and/or rigidity within the linker moiety can be used to improve overall affinities. By exploiting this design principle, related architectures with further enhanced binding affinities, as well as new photochemical properties, can be readily synthesized. Future studies will also investigate any differences in the binding selectivities of **8** – **15** and their analogues.

Experimental Section

Materials. Solvents were dried and purified using standard literature methods, whil other commercially available materials were used as received. [(tpm)Ru(dppz)Cl]PF (**2**) was prepared as described previously.[1e,8] The buffer used for UV−visible titratior consisted of 25 mM NaCl and 5 mM tris (pH 7.0) prepared with doubly distilled wate (Millipore). Calf thymus DNA (CT-DNA) was purchased from Sigma and wa sonicated for 15 minutes and subsequently purified until A_{260}/A_{280}> 1.9. Concentratior of CT-DNA solutions in terms of concentrations of base pairs were determine spectroscopically using the extinction coefficient of CT-DNA (ε = 13200 dm^3 mol cm^{-1} at 260 nm).

Instrumentation. ^{1}H NMR spectra were recorded on a Bruker AV2-400 machine. E mass spectra were obtained on a Micromass LCT ES-TOF machine, working in positiv ion mode, with m-nitrobenzyl alcohol matrix. UV-visible spectra were recorded on thermo regulated Varian-Carey 50 UV-Visible spectrometer at 25°C. Spectra wer recorded in matched quartz cells and were baseline corrected. Steady-stat luminescence emission spectra were recorded either in aerated acetonitrile or tris buffi solutions on a thermo regulated Horiba Jobin-Yvon FluoroMax-3 spectrophotomete All ITC experiments were carried out using a Microcal VP ITC microcalorimeter. Ra ITC data (see Supporting Information) were visualised using Microcal PEAQ-IT Analysis Software 1.0.0.1259 (Malvern Instruments Ltd.).

Methods. DNA viscosity experiments were carried out using published procedure UV-visible titrations were carried out in a small volume (1000 µL) 1 cm path-lengt quartz cuvette. For every data point, 2.5 µL of the solution in the cuvette was replace by 2.5 µL of a DNA stock solution. The DNA stock solution was 2.82 mM (in bas pairs) for the titrations for complexes **8** - **13** and 1.0 mM (in basepairs) for the titratior for complexes **14** and **15**. This procedure was carried out twice, once for a solution c the ligand and once for buffer only. The spectra for DNA in buffer were subsequentl subtracted from the spectra for the solutions containing both complex and DNA t obtain the corrected spectra as shown in Figure 3 and Figures S1-7. The highe absorbances before subtraction of the spectra for DNA only did not exceed 2, ensurin that the data were recorded in the range of absorbances were the instrument response linear. Titration curves at appropriate wavelengths were extracted from the correcte full spectra. The MIS model was fit to the titration curves using Origin 9.0.0 (64 bi SR2 (OriginLab Corporation). All ITC experiments were carried out at 25 °C. Comple solutions were prepared in tris buffer (5 mM Tris, 25 mM NaCl, pH 7.4) an concentrations were determined using UV-visible spectroscopy based on extinctio coefficients. The sample cell and syringe were always cleaned with ethanol followed b further cleaning with distilled water before starting any experiment. The sample ce was filled with FS-DNA solution (approximately 1.9 ml). The syringe was filled wit ligand solution (approximately 300 µl) with a concentration usually 4 fold higher tha DNA solution (exact ratios depend on individual experiments). The ligand solution wa added to the sample cell in 1 injection of 5 µl for the first addition followed by 19 injections of 15 µl each, automatically injecting every 300 seconds. During the titrations the solutions in the sample cell mixed at a stirring speed of 311 rpm. The heat effects per injection (dh) were calculated using Origin (Microcal, Inc). integrated heat effects were analysed using IC ITC and I2CITC. During the fitting routines, parameter values were restricted to the ranges below to avoid spurious numerical problems caused by unphysical parameter values, unless otherwise noted. Enthalpies are restricted to the range [-5×10^5 – $+5\times10^5$] cal mol^{-1}; equilibrium constants are restricted to the range [1 – 6×10^{20}] M^{-1} with the second equilibrium constant restricted to values smaller than the first equilibrium constant to avoid swap-overs; the stoichiometries were restricted to the range [0.0002 – 20] molecules per macromolecule unit (here base pairs).

Syntheses

N,N'-bis(4-pyridylmethyl)-1,6-hexanediamine (4py-X-4py). A solution of 4-pyridinecarboxaldehyde (18.5 g, 173 mmol) in ethanol (100 mL) was added to a solution of 1,6-hexanediamine (10.0 g, 86.6 mmol) in ethanol (200 mL) and then heated to reflux for 2 h. The reaction solution was allowed to cool to room temperature. $NaBH_4$ (8.0 g, 211 mmol) was carefully added in small portions and then the mixture was heated to reflux for 2 h and then stirred at room temperature overnight. Aqueous NaOH (2.0 M, 2 00 mL) was added to the solution. The aqueous solution was extracted with CH_2Cl_2 (3 × 200 mL), the organic fractions combined and dried over anhydrous $MgSO_4$. Filtration and concentration under reduced pressure yielded pale coloured viscous oil. On shaking with diethyl ether a cream coloured solid precipitated, which was collected by filtration, washed with copious amounts of diethyl ether and dried in vacuo (20.2 g, 74%). ^{1}H NMR (400 MHz, $CDCl_3$): δ_H = 8.49 (dd, J = 8.0, 2.8 Hz, 4H), 7.50 (d, J = 8.0 Hz, 4H), 3.82 (s, 4H), 2.64 (t, J = 6.72 Hz, 4H), 1.81 (t, J = 8.4 Hz, 4H), 1.45(m, 4H). ^{13}C NMR (63 MHz, $CDCl_3$): δ 27.1, 30.0, 49.4, 52.7, 122.9, 149.6, 149.8; ES-MS *m/z* = 299 (M*H*$^+$).

N,N'-bis(3-pyridylmethyl)-1,6-hexanediamine (3py-X-3py) was prepared in an identical manner to that above, except the 3-pyridinecarboxaldehyde was used in place of 4-pyridinecarboxaldehyde. (84.9 %); ^{1}H NMR (400 MHz, $CDCl_3$): δ_H = 8.49 (s, 2H), 8.33 (d, J = 6.0 Hz, 2H), 7.38 (m, 2H), 6.99 (m, 2H), 4.42 (s, 4H), 2.79 (m, 4H), 2.05 (s, 2H), 1.51 (m, 4H), 1.07 (m, 4H), ES-MS *m/z* = 299 (M*H*$^+$).

***N,N'*-bis(4-pyridylmethyl)-1,4-benzenedimethyleneamine (4py-Y-4py).** Benzene-1,4-dicarboxaldehyde (5.0 g, 27.3 mmol) and 4-(aminomethyl)pyridine (8.06 g, 74.6 mmol) were placed in CH_2Cl_2 (100 mL). Anhydrous $MgSO_4$ (20 g) was added to the solution and the mixture was stirred at room temperature for 24 h. The mixture was filtered and the filtrate concentrated under reduced pressure yielding the Schiff base as a golden coloured viscous oil which was not isolated. The oil was taken up in ethanol (150 mL) and $NaBH_4$ (4.0 g, 106 mmol) was added in small portions. After heating this mixture to reflux for 2 hours, it was then stirred at room temperature overnight and then aqueous NaOH (2.0 M, 200 mL) was added to the solution. The aqueous solution was extracted with CH_2Cl_2 (3×100 mL), the organic fractions combined and dried over anhydrous $MgSO_4$. Filtration and concentration under reduced pressure yielded the product as a golden coloured viscous oil which solidified into a waxy solid (9.5 g, 80%). ^{1}H NMR (400 MHz, $CDCl_3$): δ_H = 8.47 (dd, J = 6.2, 2.8 Hz, 4H), 7.28–7.22 (m,8H), 3.78 (s, 4H), 3.72 (s, 4H); ^{13}C NMR (63 MHz, $CDCl_3$): δ 51.8, 52.9, 123.0, 128.3, 138.7, 149.4, 149.8; ES-MS *m/z* = 318 (M*H*$^+$).

***N,N'*-bis(3-pyridylmethyl)-1,4-benzenedimethyleneamine (3py-Y-3py)** was prepared in an identical manner to that above, except the 3-(aminomethyl)pyridine was used in place of 4-(aminomethyl)pyridine. (80%); ^{1}H NMR (400 MHz, $CDCl_3$): δ_H = 8.52 (s, 2H), 8.35 (d, J = 6.0 Hz, 2H), 7.76 (d, J = 8.0 Hz 2H), 7.49 (m, 2H), 7.30 (s, 4H), 3.85 (s, 4H), 3.80 (s, 4H), ES-MS *m/z* = 319 (M*H*$^+$).

Synthesis of mononuclear complexes

Mononuclear complexes **8**, **10**, **12**, and **14** were prepared in an identical manner to that reported previously for **5**[10] but replacing the original linker ligand with 4py-X-4py, 4py-Y-4py, 3py-X-3py, or 3py-Y-3py, respectively.

[Ru(tpm)(dppz)(4py-X-4py)][PF_6]$_2$ (8). Orange colored solid (75%); 1H NMR (400 MHz, d6-acetone): δH = 9.84 (d, J = 8.2 Hz, 2H), 9.17 – 9.03 (m, 2H), 8.76 (s, 1H), 8.51 (m, 2H), 8.37 (t, J = 11.3 Hz, 2H), 8.23 (dd, J = 6.5, 3.4 Hz, 2H), 8.07 (dd, J = 8.3, 5.5 Hz, 4H), 7.59 – 7.40 (m, 2H), 7.27 – 7.01 (m, 4H), 6.94 – 6.76 (m, 2H), 6.46 (d, J = 2.1 Hz, 1H), 6.33 – 6.16 (m, 2H), 4.14 (s, 2H), 4.05 (s, 2H), 2.99 (t, J = 10 Hz, 2H), 2.94 (t, J = 5 Hz, 2H), 1.93 (m, 4H), 1.59(m, 4H); m/z (ES-MS) 1041 (100%, [M–PF_6]$^+$). (HRES-MS) 1041.2716 (100%, [M–PF_6]$^+$. $C_{46}H_{46}N_{14}F_6PRu$ requires 1041.2715). Elemental analysis of chloride salt calcd (%) for $C_{46}H_{46}Cl_2N_{14}Ru$•$2H_2O$: C 55.04, H 4.98, N 19.54; found: C 54.94; H 4.39; N 15.59;

[Ru(tpm)(dppz)(4py-Y-4py)][PF_6]$_2$ (10). Orange colored solid (56%); **^{1}H NMR (400 MHz, d_6-acetone):** δ_H = 9.84 (d, J = 7.1 Hz, 2H), 9.02 (dd, J = 6.6, 3.3 Hz, 2H), 8.86 (s, 1H), 8.74 – 8.50 (m, 4H), 8.50 – 8.35 (m, 4H), 8.23 (dd, J = 6.5, 3.4 Hz, 4H), 8.12 – 7.94 (m, 2H), 7.73 (dd, J = 3.7, 7.0 Hz, 4H), 7.60 (s, 4H), 7.58 – 7.31 (m, 4H), 6.84 (d, J = 2.4 Hz, 1H), 4.25 (m, 2H), 4.11 (s, 2H), 3.14 – 3.02 (m, 4H); *m/z* (ES-MS) 1061 (100%, [M –PF_6]$^+$). HRES-MS: 1061.2435 (100%, [M –PF_6]$^+$. $C_{48}H_{42}N_{14}F_6PRu$ requires 1061.2402). Elemental analysis of chloride salt calcd (%) for $C_{48}H_{42}Cl_2N_{14}Ru$•H_2O: C 57.31, H 4.37, N 19.50; found: C 57.26; H 4.30; N 19.47;

[Ru(tpm)(dppz)(3py-X-3py)][PF_6]$_2$ (12). Red-orange coloured solid (63.3 %); **^{1}H NMR (400 MHz, CD_3CN):** δH = 10.06 (s, 1H), 9.81 (d, J = 8.2 Hz, 2H), 9.10 (d, J = 5.5 Hz, 2H), 8.67 (d, J = 5.3 Hz, 2H), 8.48 (d, J = 2.8 Hz, 2H), 8.20 (m, 2H), 7.87 (m, 2H), 7.82 (m, 2H), 7.48 (dd, J = 10 Hz, 4 Hz, 2H), 7.38 (m, 2H), 7.06 (dd, J = 4.4, 1.4 Hz, 2H), 6.83 (t, J = 4 Hz, 2H). 6.79 (m, 2H), 6.44 (d, J = 2.2 Hz, 2H), 6.29 – 6.14 (m, 1H), 4.34 (s, 2H), 3.53 (s, 2H), 2.98 (m, 2H), 1.97 (m, 2H), 1.50 (dt, J = 4.9, 2.5 Hz, 4H), 1.36 (m, 4H);; *m/z* (ES-MS) 1041 (100% [M-PF_6]$^+$). HRES-MS: 1041.2710 (100% [M-PF_6]$^+$. $C_{46}H_{46}N_{14}F_6PRu$ requires 1041.2726). calcd (%) for $C_{46}H_{46}F_{12}N_{14}P_2Ru$•$H_2O$: C 45.85, H 3.98, N 16.28; found: C 45.62, H 3.81, N 16.57

[Ru(tpm)(dppz)(3py-Y-3py)][PF_6]$_2$ (14). Orange coloured solid (65%); **^{1}H NMR (400 MHz, CD_3CN):** δ_H = 9.81 (d, J = 7.6 Hz, 2H), 9.13 (s,1H), 9.08 (d, J = 4.7 Hz, 2H), 8.63 (t, J = 7.8 Hz, 2H), 8.60 (d, J = 2.4 Hz, 2H), 8.57 (m, 2H), 8.41 (d, J = 2.5 Hz, 2H), 8.21 (m, 2H), 8.06 (d, J = 2.8 Hz, 2H), 7.85 (d, J = 8 Hz, 2H), 7.56 (m, 4H), 7.36 (d, J = 6 Hz, 2H), 7.05 (t, J = 8 Hz, 2H), 6.80 (t, J = 2.3 Hz, 2H), 6.38 (d, J = 2.0 Hz, 2H), 6.17 (t, J = 8.4 Hz, 1H) 2.60 (s, 2H), 2.55 (m, 2H), 1.59 (m, 2H), 1.52 (m, 2H);; *m/z* (ES-MS) 1061 (100%, [M –PF_6]$^+$). HRES-MS: 1061.2397 (100%, [M –PF_6]$^+$. $C_{48}H_{42}N_{14}F_6PRu$ requires 1061.2444). calcd (%) for $C_{48}H_{42}F_{12}N_{14}P_2Ru$•$3H_2O$: C 45.71, H 3.80, N 15.55; found: C 45.69, H 3.69, N 15.42

Synthesis of dinuclear complexes

The dinuclear complexes were synthesised through a method adopted from that reported for complex **6**, illustrated by the detailed procedure used for complex **9**. Like many polyamines such as spermine derivatives these complexes are hygroscopic[76] so that rigorously dried samples rapidly absorb water, therefore consistent elemental analyses were only obtained through exposure to the atmosphere until weight changes no longe occurred.

[{(tpm)Ru(dppz)}$_2$(4py-X-4py)][(PF_6)$_4$] (9). [(tpm)Ru(dppz)(Cl)]PF_6 (65 mg, 0.0 mmol) and $AgNO_3$ (120 mg, 0.70 mmol) were placed in a 1:1 mixture of ethanol an water (40 mL) and heated to reflux for 2 h. The solution was allowed to cool an filtered through celite to remove the AgCl precipitate. The filtrate was returned to th reaction vessel. [8][(PF_6)$_2$] (360 mg, 0.3 mmol) in acetone (15 mL) was added and th solution was refluxed for 72 h. The solution was allowed to cool to room temperatur Purification was achieved via ion-exchange chromatography on Sephadex CM-25 resi eluting with water acetone mixtures (5:3) with increasing concentrations of NaC Monomeric complexes were eluted with 0.05 M NaCl and the desired bimetall complex was eluted with 0.1–0.2 M NaCl in water:acetone (5:3). A concentrate aqueous solution of NH_4PF_6 (~10 mL) was added to the filtrate. On concentration i vacuo, the bimetallic complex precipitated. It was collected by centrifugation, washe with copious amounts of water and dried in vacuo producing the title compound in 48 yield. λ_{max}(CH_3CN)/nm 276 (ε/dm^3 mol^{-1} cm^{-1} 100 300), 318 (29 600), 355 (25 900 368 (23 000), 468 (7 700); ^{1}H NMR (400 MHz, d_6-acetone): δ_H = 10.09 (s, 2H), 9.8 (dd, J = 3.0, 2.3,Hz, 4H), 9.11 (dd, J = 1.3, 5.8 Hz, 4H), 8.97 (d, J = 2.4 Hz, 2H), 8.77 8.49 (m, 4H), 8.38 (dd, J = 4.1, 2.9 Hz, 4H), 8.38 – 8.10 (m, 4H), 8.10 – 7.97 (m, 4H 7.66 – 7.42 (m, 6H), 7.09 (t, J = 6.3 Hz, 2H), 6.96 – 6.75 (m, 4H), 6.64 (d, J = 2.3 H 2H), 6.34 – 6.21 (m, 2H), 4.28 (s, 4H), 3.38 (m,4H), 1.82 (m, 8H), 1.58 (m, 4H); (ES MS) 892 (100%, [M –2PF_6]$^{2+}$). HRES-MS: 892.1607 (100%, [M –2PF_6]^2 $C_{74}H_{66}N_{24}F_{12}P_2Ru_2$ requires 892.1636). calcd (%) for $C_{74}H_{66}F_{24}N_{24}P_4Ru_2$•$3H_2O$: 41.74, H 3.38, N 15.79; found: C 41.22, H 3.45, N 15.86

[{(tpm)Ru(dppz)}$_2$(4py-Y-4py)][(PF_6)$_4$] (11) was prepared in an identical manner t that above, except the monomeric complex **[10]**[(PF_6)$_2$] was used in place **[8]**[(PF_6)$_2$]. (45%) **^{1}H NMR (400 MHz, d_6-acetone):** δ_H = 9.96 (s, 2H), 9.90 – 9.74 (n 4H), 9.64 (d, J = 8.1 Hz, 4H), 9.30 – 9.00 (m, 4H), 8.59 (dd, J = 3.7, 2.5 Hz, 4H), 8.39 J = 2.3 Hz, 2H), 8.28 (d, J = 4.0 Hz, 4H), 8.19 – 7.99 (m, 4H), 7.68 (d, J = 3.3 Hz, 4H 7.44 (t, J = 2.1 Hz, 4H), 7.13 (d, J = 5.8 Hz, 4H), 7.13 – 6.92 (m, 4H), 6.87 – 6.57 (n 4H), 6.57 – 6.37 (m, 2H), 6.19 (t, J = 1.7 Hz, 2H), 4.06 (s, 4H), 3.30 (s,4H); HRES-MS 902.7491 (100%, [M –2PF_6]$^{2+}$. $C_{76}H_{62}F_{12}N_{24}P_2Ru_2$ requires 902.7462); elementa analysis of chloride calcd (%) for $C_{76}H_{62}Cl_4N_{24}Ru_2$•$6H_2O$: C 51.71, H 4.19, N 19.0 found: C 51.42, H 4.25, N 19.81; m/z (ES-MS) 901 (100%, [M –2PF_6]$^{2+}$).

[{(tpm)Ru(dppz)}$_2$(3py-X-3py)][(PF_6)$_4$] (13) was prepared in an identical manner t that above, except the monomeric complex [**12**][(PF_6)$_2$] was used in place of [**8**][(PF_6) (60%). **^{1}H NMR (400 MHz, CD_3CN):** δ_H = 9.83 (dd, J = 8.2, 1.2 Hz, 4H), 9.21 (s, 2H 9.10 (d, J = 5.6 Hz, 2H), 8.38 (d, J = 2.8 Hz, 4H), 8.27 (m, 6H), 8.12 (s, 2H), 8.02 (n 2H), 7.81 (dd, J = 9.9, 4.2 Hz, 8H), 7.67 (dd, J = 7.8, 6.0 Hz, 4H), 7.50 (m, 4H), 7.25 (J = 1.6 Hz, 2H), 6.86 (t, J = 4 Hz, 6H) 6.40 (m, 2H), 3.47 (s, 4H), 2.79 (m, 4H), 1.83 (r 4H), 1.76 (m, 4H); m/z (ES-MS) 892 (100%, [M –2PF_6]$^{2+}$). HRES-MS: 892.163 (100%, [M –2PF_6]$^{2+}$. $C_{74}H_{66}N_{24}F_{12}P_2Ru_2$ requires 892.1631). calcd (%) fo $C_{74}H_{66}F_{24}N_{24}P_4Ru_2$•$2H_2O$: C 42.09, H 3.31, N 15.92; found: C 42.60, H 3.39, N 15.31

[{(tpm)Ru(dppz)}$_2$(3py-Y-3py)][(PF_6)$_4$] (15) was prepared in an identical manner t that above, except the monomeric complex [**14**][(PF_6)$_2$] was used in place of [**8**][(PF_6)$_2$]. (56 %): **^{1}H NMR (400 MHz, CD_3CN):** δ_H = 9.79 (dd, J = 7.9, 2.5 Hz, 4H), 9.21 (m, 2H), 9.10 (s, 2H), 8.64 (m, 4H), 8.53 (t, J = 4.9 Hz, 4H), 8.36 (t, J = 4.9 Hz, 4H), 8.20 (s, 2H), 8.17 (m, 2H), 7.96 (m, 4H), 7.80 (m, 4H), 7.62 (d, J = 2.3 Hz, 4H), 7.28 (m, 2H), 7.08 (s, 4H), 6.81 (m, 4H), 6.62 (d, J = 2.3 Hz, 4H) 6.28 (m, 2H) 2.97 (s, 4H), 2.73 (m, 4H); m/z (ES-MS) 902 (100%, [M –2PF_6]$^{2+}$). HRES-MS: 902.1474 (100%, [M –2PF_6]$^{2+}$. $C_{76}H_{62}F_{12}N_{24}P_2Ru_2$ requires 902.1511); elemental analysis calcd (%) for $C_{76}H_{62}F_{12}N_{24}P_4Ru_2$•$6H_2O$: C 41.42, H 3.36, N 15.26; found: C 41.33, H 3.05, N 15.79.

Acknowledgements

A special thanks to the KRG-Scholarship 'Human Capacity Development Program (HCDP)' for the financial support provided to both HKS and IQS.

[1] K. E. Erkkila, D. T. Odom, J. K. Barton, *Chem. Rev.* **1999**, *99*, 2777–2796.

[2] C. Metcalfe, J. A. Thomas, *Chem Soc Rev* **2003**, *32*, 215–224.

[3] B. M. Zeglis, V. C. Pierre, J. K. Barton, *Chem. Commun.* **2007**, 4565–4579.

[4] F. R. Keene, J. A. Smith, J. G. Collins, *Coord. Chem. Rev.* **2009**, *253*, 2021–2035.

[5] K. K.-W. Lo, M.-W. Louie, K. Y. Zhang, *Coord. Chem. Rev.* **2010**, *254*, 2603–2622.

[6] A. W. McKinley, P. Lincoln, E. M. Tuite, *Coord. Chem. Rev.* **2011**, *255*, 2676–2692.

[7] Q. Zhao, C. Huang, F. Li, *Chem Soc Rev* **2011**, *40*, 2508.

[8] E. Baggaley, J. A. Weinstein, J. A. Williams, *Coord. Chem. Rev.* **2012**, *256*, 1762–1785.

[9] X. Wang, Z. Guo, *Chem Soc Rev* **2013**, *42*, 202–224.

[10] M. Mauro, A. Aliprandi, D. Septiadi, N. S. Kehr, L. De Cola, *Chem Soc Rev* **2014**, *43*, 4144.

[11] A. E. Friedman, J. C. Chambron, J. P. Sauvage, N. J. Turro, J. K. Barton, *J. Am. Chem. Soc.* **1990**, *112*, 4960–4962.

[12] M. R. Gill, J. A. Thomas, *Chem Soc Rev* **2012**, *41*, 3179–3192.

[13] G. Li, L. Sun, L. Ji, H. Chao, *Dalton Trans* **2016**, *45*, 13261–13276.

[14] Y. Jenkins, A. E. Friedman, N. J. Turro, J. K. Barton, *Biochemistry* **1992**, *31*, 10809–10816.

[15] C. Hiort, P. Lincoln, B. Nordén, *J. Am. Chem. Soc.* **1993**, *115*, 3448–3454.

[16] I. Haq, P. Lincoln, D. Suh, B. Nordén, B. Z. Chowdhry, J. B. Chaires, *J. Am. Chem. Soc.* **1995**, *117*, 4788–4796.

[17] C. M. Dupureur, J. K. Barton, *Inorg Chem* **1997**, *36*, 33–43.

[18] E. Tuite, P. Lincoln, B. Nordén, *J. Am. Chem. Soc.* **1997**, *119*, 239–240.

[19] P. Lincoln, E. Tuite, B. Nordén, *J. Am. Chem. Soc.* **1997**, *119*, 1454–1455.

[20] S. J. Franklin, C. R. Treadway, J. K. Barton, *Inorg Chem* **1998**, *37*, 5198–5210.

[21] J. P. Hall, K. O'Sullivan, A. Naseer, J. A. Smith, J. M. Kelly, C. J. Cardin, *Proc Natl Acad Sci USA* **2011**, *108*, 17610–17614.

[22] H. Song, J. T. Kaiser, J. K. Barton, *Nat Chem* **2012**, *4*, 615–620.

[23] H. Niyazi, J. P. Hall, K. O'Sullivan, G. Winter, T. Sorensen, J. M. Kelly, C. J. Cardin, *Nat Chem* **2012**, *4*, 621–628.

[24] J. P. Hall, H. Beer, K. Buchner, D. J. Cardin, C. J. Cardin, *Organometallics* **2015**, 150506104229009.

[25] J. P. Hall, D. Cook, S. R. Morte, P. McIntyre, K. Buchner, H. Beer, D. J. Cardin, J. A. Brazier, G. Winter, J. M. Kelly, et al., *J. Am. Chem. Soc.* **2013**, *135*, 12652–12659.

[26] C. Metcalfe, H. Adams, I. Haq, J. A. Thomas, *Chem. Commun.* **2003**, 1152–1153.

[27] F. O'Reilly, J. Kelly, A. Kirsch-De Mesmaeker, *Chem. Commun.* **1996**, 1013–1014.

[28] F. F. Leng, W. Priebe, J. B. Chaires, *Biochemistry* **1998**, *37*, 1743–1753.

[29] Y. Qu, N. Farrell, *Inorg Chem* **1995**, *34*, 3573–3576.

[30] M. J. Hannon, V. Moreno, M. J. Prieto, E. Moldrheim, E. Sletten, I. Meistermann, C. J. Isaac, K. J. Sanders, A. Rodger, *Angew. Chem. Int. Ed. Engl.* **2001**, *40*, 880–884.

[31] G. I. Pascu, A. C. G. Hotze, C. Sanchez-Cano, B. M. Kariuki, M. J. Hannon, *Angew. Chem. Int. Ed.* **2007**, *46*, 4374–4378.

[32] V. Gonzalez, T. Wilson, I. Kurihara, A. Imai, J. A. Thomas, J. Otsuki, *Chem. Commun. (Camb.)* **2008**, 1868–1870.

[33] U. McDonnell, J. M. C. A. Kerchoffs, R. P. M. Castineiras, M. R. Hicks, A. C. G. Hotze, M. J. Hannon, A. Rodger, *Dalton Trans* **2008**, 667.

[34] K. Suntharalingam, A. J. P. White, R. Vilar, *Inorg Chem* **2010**, *49*, 8371–8380.

[35] A. Medina-Molner, B. Spingler, *Chem. Commun.* **2012**, *48*, 1961.

[36] D. L. Ang, B. W. J. Harper, L. Cubo, O. Mendoza, R. Vilar, J. Aldrich-Wright, *Chem. Eur. J.* **2015**, *22*, 2317–2325.

[37] S. Mardanya, S. Karmakar, D. Mondal, S. Baitalik, *Inorg Chem* **2016**, *55*, 3475–3489.

[38] J. L. Morgan, C. B. Spillane, J. A. Smith, D. P. Buck, J. G. Collins, F. R. Keene, *Dalton Trans* **2007**, 4333.

[39] F. Li, Y. Mulyana, M. Feterl, J. M. Warner, J. G. Collins, F. R. Keene, *Dalton Trans* **2011**, *40*, 5032.

[40] M. J. Pisani, P. D. Fromm, Y. Mulyana, R. J. Clarke, H. Körner, K. Heimann, J. G. Collins, F. R. Keene, *ChemMedChem* **2011**, *6*, 848–858.

[41] F. Li, E. J. Harry, A. L. Bottomley, M. D. Edstein, G. W. Birrell, C. E. Woodward, F. R. Keene, J. G. Collins, *Chem. Sci.* **2014**, *5*, 685–693.

[42] F. Li, J. G. Collins, F. R. Keene, *Chem Soc Rev* **2015**, *44*, 2529–2542.

[43] J. Aldrich-Wright, C. Brodie, E. C. Glazer, N. W. Luedtke, L. Elson-Schwab, Y Tor, *Chem. Commun.* **2004**, 1018.

[44] C.-C. Ju, A.-G. Zhang, C.-L. Yuan, X.-L. Zhao, K.-Z. Wang, *J. Inorg. Biochem* **2011**, *105*, 435–443.

[45] P. Liu, B.-Y. Wu, J. Liu, Y.-C. Dai, Y.-J. Wang, K.-Z. Wang, *Inorg Chem* **201** *55*, 1412–1422.

[46] B. Önfelt, P. Lincoln, B. Nordén, *J. Am. Chem. Soc.* **1999**, *121*, 10846–10847.

[47] B. Önfelt, P. Lincoln, B. Nordén, *J. Am. Chem. Soc.* **2001**, *123*, 3630–3637.

[48] L. M. Wilhelmsson, F. Westerlund, P. Lincoln, B. Nordén, *J. Am. Chem. So* **2002**, *124*, 12092–12093.

[49] P. Nordell, P. Lincoln, *J. Am. Chem. Soc.* **2005**, *127*, 9670–9671.

[50] D. R. Boer, L. Wu, P. Lincoln, M. Coll, *Angew. Chem. Int. Ed.* **2014**, *53*, 1949 1952.

[51] L. Wu, A. Reymer, C. Persson, K. Kazimierczuk, T. Brown, P. Lincoln, I Nordén, M. Billeter, *Chem. Eur. J.* **2013**, *19*, 5401–5410.

[52] A. A. Almaqwashi, J. Andersson, P. Lincoln, I. Rouzina, F. Westerlund, M. C Williams, *Biophysj* **2016**, *110*, 1255–1263.

[53] P. Nordell, F. Westerlund, L. M. Wilhelmsson, B. Nordén, P. Lincoln, *Angev Chem. Int. Ed.* **2007**, *46*, 2203–2206.

[54] C. Metcalfe, M. Webb, J. A. Thomas, *Chem. Commun.* **2002**, 2026–2027.

[55] C. Metcalfe, I. Haq, J. A. Thomas, *Inorg Chem* **2004**, *43*, 317–323.

[56] S. P. Foxon, T. Phillips, M. R. Gill, M. Towrie, A. W. Parker, M. Webb, J. A Thomas, *Angew. Chem. Int. Ed. Engl.* **2007**, *46*, 3686–3688.

[57] P. Waywell, V. Gonzalez, M. R. Gill, H. Adams, A. J. H. M. Meijer, M. I Williamson, J. A. Thomas, *Chem. Eur. J.* **2010**, *16*, 2407–2417.

[58] M. G. Walker, V. Gonzalez, E. Chekmeneva, J. A. Thomas, *Angew. Chem. In Ed. Engl.* **2012**, *51*, 12107–12110.

[59] M. H. Hou, S. B. Lin, J. Yuann, W. C. Lin, A. Wang, L. S. Kan, *Nucleic acid Research* **2001**, *29*, 5121–5128.

[60] J. Dyer, W. J. Blau, C. G. Coates, C. M. Creely, J. D. Gavey, M. W. George, I C. Grills, S. Hudson, J. M. Kelly, P. Matousek, et al., *Photochem. Photobio Sci.* **2003**, *2*, 542.

[61] C. G. Coates, J. J. McGarvey, P. L. Callaghan, M. Coletti, J. G. Hamilton, *Phys. Chem. B* **2001**, *105*, 730–735.

[62] S. J. Moon, J.-M. Kim, J. Y. Choi, S. K. Kim, J. S. Lee, H. G. Jang, *J. Inorg Biochem.* **2005**, *99*, 994–1000.

[63] J.-M. Kim, J.-M. Lee, J. Y. Choi, H. M. Lee, S. K. Kim, *J. Inorg. Biochem.* **2007**, *101*, 1386–1393.

[64] D. A. Lutterman, A. Chouai, Y. Liu, Y. Sun, C. D. Stewart, K. R. Dunbar, C. Turro, *J. Am. Chem. Soc.* **2008**, *130*, 1163–1170.

[65] J. D. J. McGhee, P. H. P. von Hippel, *J. Mol. Biol.* **1974**, *86*, 469–489.

[66] L. Hahn, N. J. Buurma, L. H. Gade, *Chem. Eur. J.* **2016**, *22*, 6314–6322.

[67] G. Cohen, H. Eisenberg, *Biopolymers* **1969**, *8*, 45–55.

[68] L. Kapicak, E. J. Gabbay, *J. Am. Chem. Soc.* **1975**, *97*, 403–408.

[69] S. Satyanarayana, J. C. Dabrowiak, J. B. Chaires, *Biochemistry* **1992**, *31*, 9319–9324.

[70] R. T. Wheelhouse, N. C. Garbett, N. J. Buurma, J. B. Chaires, *Angew. Chem. Int. Ed.* **2010**, *49*, 3207–3210.

[71] R. S. Spolar, J. R. Livingstone, M. T. Record, *Biochemistry* **1992**, *31*, 3947–3955.

[72] N. J. Buurma, I. Haq, *Methods* **2007**, *42*, 162–172.

[73] N. J. Buurma, I. Haq, *J. Mol. Biol.* **2008**, *381*, 607–621.

[74] J. B. Chaires, *Archives of Biochemistry and Biophysics* **2006**, *453*, 26–31.

[75] J. B. Chaires, *Annu. Rev. Biophys.* **2008**, *37*, 135–151.

[76] J.-G. Delcros, S. Tomasi, S. Carrington, B. Martin, J. Renault, I. S. Blagbrough, P. Uriac, *J. Med. Chem.* **2002**, *45*, 5098–5111.

Received: ((will be filled in by the editorial staff))
Revised: ((will be filled in by the editorial staff))
Published online: ((will be filled in by the editorial staff))

10.1002/chem.201605750

Entry for the Table of Contents (Please choose one layout only)

Layout 1:

Strengthened links

Hiwa K Saeed, Ibrahim Q Saeed, Niklaas J Buurma, and Jim A. Thomas……..…… Page – Page

The structure of linkers affects the DNA binding properties of tethered dinuclear ruthenium (II) metallo-intercalators

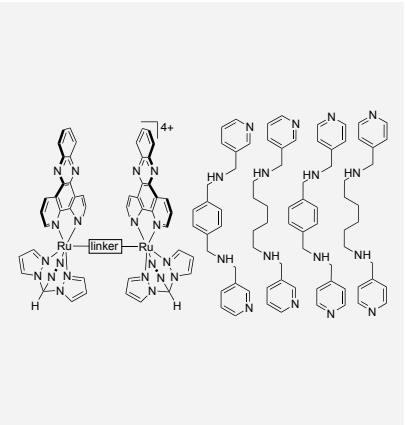

The DNA binding properties of non-threading dinuclear Ru^{II}(dppz).bis-intercalators are highly dependent on the nature of their linker ligand. Judicious selection of the connectivity and structure of the tether enhances binding by two orders of magnitude compared to previously reported systems